

## Suitability of the double Langevin function for description of anhysteretic magnetization curves in NO and GO electrical steel grades

Simon Steentjes, Martin Petrun, Gregor Glehn, Drago Dolinar, and Kay Hameyer

Citation: *AIP Advances* **7**, 056013 (2017); doi: 10.1063/1.4975135

View online: <http://dx.doi.org/10.1063/1.4975135>

View Table of Contents: <http://aip.scitation.org/toc/adv/7/5>

Published by the [American Institute of Physics](#)

---

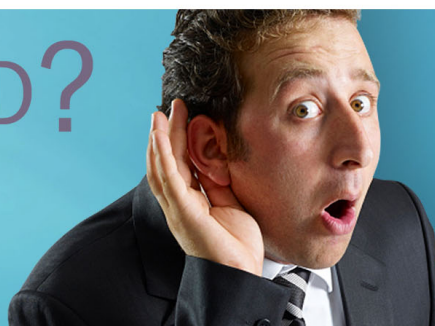
---

# HAVE YOU HEARD?

Employers hiring scientists and  
engineers trust

**PHYSICS TODAY | JOBS**

[www.physicstoday.org/jobs](http://www.physicstoday.org/jobs)



# Suitability of the double Langevin function for description of anhysteretic magnetization curves in NO and GO electrical steel grades

Simon Steentjes,<sup>1</sup> Martin Petrun,<sup>2</sup> Gregor Glehn,<sup>1</sup> Drago Dolinar,<sup>2</sup> and Kay Hameyer<sup>1</sup>

<sup>1</sup>*Institute of Electrical Machines, RWTH Aachen University, D-52062 Aachen, Germany*

<sup>2</sup>*Institute of Power Engineering, FERI, University of Maribor, SI-2000 Maribor, Slovenia*

(Presented 1 November 2016; received 23 September 2016; accepted 4 November 2016; published online 26 January 2017)

This paper compares the match obtained using the classical Langevin function, the tanh function as well as a recently by the authors proposed double Langevin function with the measured anhysteretic magnetization curve of three different non-oriented electrical steel grades and one grain-oriented grade. Two standard non-oriented grades and a high-silicon grade (Si content of 6.5%) made by CVD are analyzed. An excellent match is obtained using the double Langevin function, whereas the classical solutions are less appropriate. Thereby, problems such as those due to propagation of approximation errors observed in hysteresis modeling can be bypassed. © 2017 Author(s). All article content, except where otherwise noted, is licensed under a Creative Commons Attribution (CC BY) license (<http://creativecommons.org/licenses/by/4.0/>). [<http://dx.doi.org/10.1063/1.4975135>]

## I. INTRODUCTION

Many of the most used and well-known hysteresis models exploit the Langevin function for description of the anhysteretic magnetization curves of different materials. Among these models is for example the Jiles-Atherton<sup>1</sup> or the GRUCAD<sup>2</sup> hysteresis model. Although the Langevin function exhibits some interesting advantages over other functions, it was, e.g., selected quite arbitrarily in the process of deriving the Jiles-Atherton hysteresis model.<sup>3</sup> Based on these advantages, the Langevin function emerged as the most popular choice to describe the anhysteretic part of many contemporary hysteresis models.

Using the Langevin function when predicting hysteresis loops can however also lead to problems that are linked to the limited number of parameters and accuracy of the description of the anhysteretic curve.<sup>3,4</sup> The inability of describing a measured anhysteretic curve accurately prevents adequate parameter identification and consequently accurate prediction of static hysteresis loops. The biggest deviations arise especially in the knee region of the anhysteretic curve. This leads further on to bigger deviations when using discussed hysteresis models to predict dynamic magnetization and power losses in soft magnetic materials. In this paper these problems are addressed by applying a double Langevin function instead of single one, as it is common practice. The double Langevin function enables to improve the accuracy of the description of various anhysteretic magnetization curves and, at the same time, the parameters are linked to the material microstructure and alloy, i.e., physical-based.

## II. THEORETICAL BACKGROUND

The aim is to derive a parametric saturation curve that describes the anhysteretic magnetization curve  $J_{an}(H)$  given by (1) in soft magnetic materials. For this purpose a soft magnetic material lamination is considered as a multi-domain system composed of an array of pseudo-domains with fixed domain walls. This allows introducing a characteristic field  $H_0$  (2) in the Boltzmann statistics, which can be related to the density of magnetic moments per mean domain width.<sup>5</sup>

$$\frac{J_{\text{an}}(H)}{J_s} = f_{\text{an}}\left(\frac{H}{H_0}\right) \quad (1)$$

$$H_0 = \frac{k_B T}{\mu_0 M_s N} \quad (2)$$

The characteristic magnetic field strength  $H_0$  (2) is proportional to temperature  $T$ , domain density  $N$  and the inverse of the saturation magnetization  $M_s$ . The domain density  $N$  is considered to be constant because only reversible changes along the anhysteretic (thermodynamic equilibrium) path are considered which can only involve rotation of domain moments. The characteristic field should be treated as a constant of the material, which is dependent on the microstructure and texture.

Starting from the quantum-mechanical Brillouin function two expressions for the anhysteretic magnetization curve can be obtained in the limit,  $\mathcal{J} = 1/2$  and  $\mathcal{J} \rightarrow \infty$ , where  $\mathcal{J}$  is the internal quantum number. The Brillouin function reduces to the Langevin function in the limit  $\mathcal{J} \rightarrow \infty$ , i.e., the magnetic moments can take any direction (classical model). For  $\mathcal{J} = 1/2$  the magnetic moment is due entirely spin without any orbital contribution the Brillouin function reduces to tanh-function. The Langevin function (3) describes magnetic saturation based on statistical mechanics reasoning in classical Boltzmann statistics

$$\frac{J_{\text{an}}(H)}{J_s} = \coth\left(\frac{H}{H_0}\right) - \frac{H_0}{H} \quad (3)$$

The tanh-function is given by:

$$\frac{J_{\text{an}}(H)}{J_s} = \tanh\left(\frac{H}{H_0}\right) \quad (4)$$

These scalar expressions were originally derived for paramagnets. But treating the ferromagnet as an assembly of pseudo-domains with chains of collinear magnetic moments<sup>5</sup> is possible by introduction of the aforementioned characteristic magnetic field strength  $H_0$ .

In addition to the Langevin- and tanh-function, in this paper a linear combination of two different Langevin functions (5) originally proposed by the authors in Refs. 6 and 7, which gives also an anhysteretic function, is used as a parametric saturation curve in soft magnetic materials to represent the region of the anhysteretic curve, where the motion of Bloch walls is dominating, and the region, where the rotation of the magnetic moments relative to the preferred axis (coherent rotation) occurs. Both share the property that their slopes at  $H = 0$  A/m are maximal and, as a result, this relates also to their linear combination.<sup>3</sup> The two passages of magnetization can be observed in the measurements (Figs. 1(b), 3(b), 5(b) and 7(b)).

$$J_{\text{an}}(H) = J_{s,a} \left[ \coth\left(\frac{H}{H_{0,a}}\right) - \frac{H_{0,a}}{H} \right] + J_{s,b} \left[ \coth\left(\frac{H}{H_{0,b}}\right) - \frac{H_{0,b}}{H} \right] \quad \text{with} \quad J_s = J_{s,b} + J_{s,a} \quad (5)$$

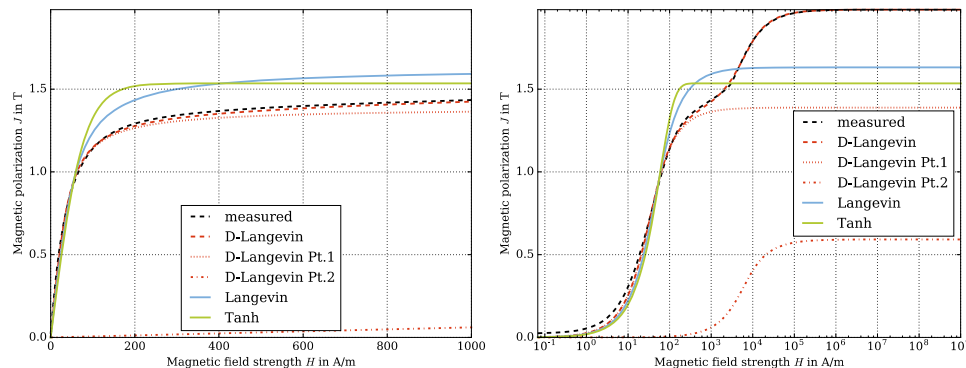


FIG. 1. Comparison of measured (black dashed line) and modelled anhysteretic magnetization curves of grade M235-35A. (a) Normal scaling and (b) log-scale on abscissa. In addition, the two components of the double Langevin function (Pt. 1 and 2) are shown.

In (5) the term indexed with Pt.1, i.e., index a, represents the magnetic polarization due to the motion of Bloch walls, and the term indexed with Pt.2, i.e., index b, represents the magnetic polarization, occurring at higher field intensity, due the eventual rotation of the magnetic moments out of the easy magnetization axes. The contribution of both adds to the saturation magnetic polarization of the material, which is defined by the alloy content. This expression is very accurate and delivers a convenient tool to accurately represent the anhysteretic curve with a smooth easily differentiable function.

### III. RESULTS

Three different soft magnetic materials, classified as M235-35A, M400-50A and JNEX-900 (thickness 0.1 mm), were characterized using an Epstein frame under quasi-static excitations. Therefore, the magnetizing field is changed in a continuous fashion, as slowly as reasonable to avoid eddy-current effects. The quasi-static hysteresis loop is identified by cycling the magnetic field continuously from the maximum positive to the maximum negative value and back. This then allows identifying the anhysteretic curve.

Figs. 1 and 2 show comparisons of the measured data and the three different functions for representing the anhysteretic magnetization for grade M235-35A, whereas Table I gives the identified parameters. These were obtained by matching the three different functions (1), (3) and (5) with the measured data to reduce the least square error. The saturation values of the two double Langevin are constrained to sum up to the saturation magnetic polarization. This is identified from the alloy content as 1.98 T for M235-35A, 2.01 T for M400-50A, 1.80 T for JNEX-900. Fig. 2(b) gives the match of the magnetic susceptibility.

The introduction of one additional degree of freedom significantly increases the accuracy of the representation of the anhysteretic curve. Further on, the shape of the measured anhysteretic curve clearly shows the two passages of the magnetization process. From 0 to 1.4 T and from 1.4 T to  $J_s = 1.98$  T, which resemble the parameters of the two Langevin functions (Table I). Merely in the region of small magnetic field strength some small deviations occur (Fig. 2).

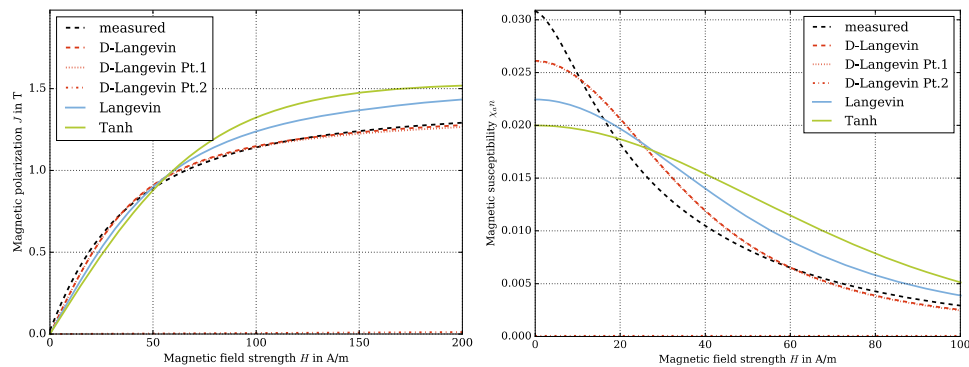


FIG. 2. Comparison of measured (black dashed line) and modelled anhysteretic magnetization curves of grade M235-35A. (a) Zoom of Fig. 1 and (b) magnetic susceptibility. In addition, the two components of the double Langevin function (Pt. 1 and 2) are shown.

TABLE I. Parameters of the Anhysteretic Function for Grade M235-35A.

$f_{an}$	$J_{s,a}$ in T	$H_{0,a}$ in A/m	$J_{s,b}$ in T	$H_{0,b}$ in A/m
Langevin	1.63098	24.2185	–	–
Tanh	1.53454	76.7888	–	–
Double Langevin	1.38791	17.7596	0.592095	3205.88

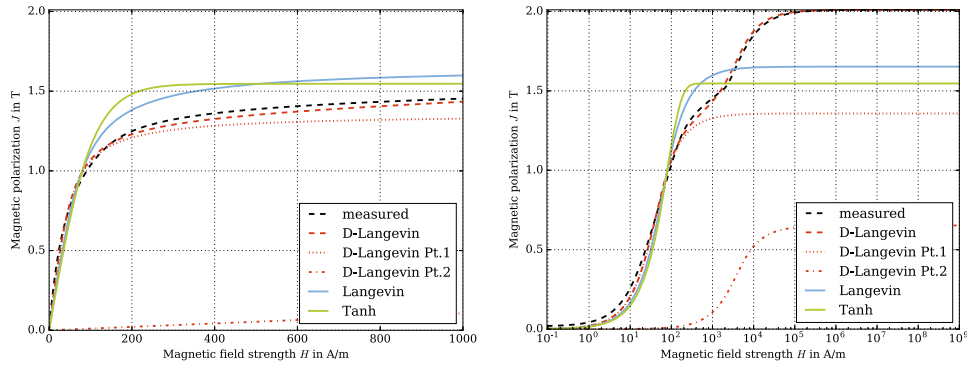


FIG. 3. Comparison of measured (black dashed line) and modelled an hysteretic magnetization curves of grade M400-50A. (a) Normal scaling and (b) log-scale on abscissa. In addition, the two components of the double Langevin function (Pt. 1 and 2) are shown.

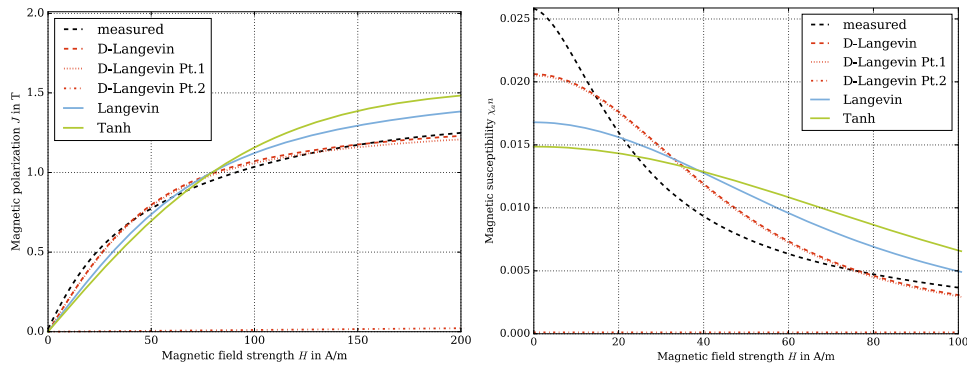


FIG. 4. Comparison of measured (black dashed line) and modelled an hysteretic magnetization curves of grade M400-50A. (a) Zoom of Fig. 1 and (b) magnetic susceptibility. In addition, the two components of the double Langevin function (Pt. 1 and 2) are shown.

Similar accuracy can be obtained for the M400-50A grade with lower silicon content (Figs. 3 and 4). The parameters are given in Table II. Again the two stages in the magnetization process are apparent, which are reproduced by the superposition of the Langevin functions. In contrast, the classical Langevin- and tanh-function with two degrees of freedom, i.e., interpreting the saturation polarization as a parameter are less appropriate over the whole polarization range.

The application of the double Langevin function to a high-silicon grade with 6.5 % silicon uniformly distributed in the sheet and a saturation polarization of 1.8 T is shown in Figs. 5 and 6. The corresponding parameters are given in Table III. It is apparent that the classical Langevin- and tanh-function with two degrees of freedom can appropriately describe the first region of the magnetization curve up to 1.0 T, but do not represent the material saturation correctly. In contrast, the double Langevin function with one additional degree of freedom is able to represent both passages. A small offset between the two passages is apparent (1.15 T to 1.5 T). In contrast to the two standard

TABLE II. Parameters of the An hysteretic Function for Grade M400-50A.

$f_{an}$	$J_{s,a}$ in T	$H_{0,a}$ in A/m	$J_{s,b}$ in T	$H_{0,b}$ in A/m
Langevin	1.65246	32.7991	–	–
Tanh	1.54634	104.041	–	–
Double Langevin	1.35749	22.0601	0.652514	2016.98

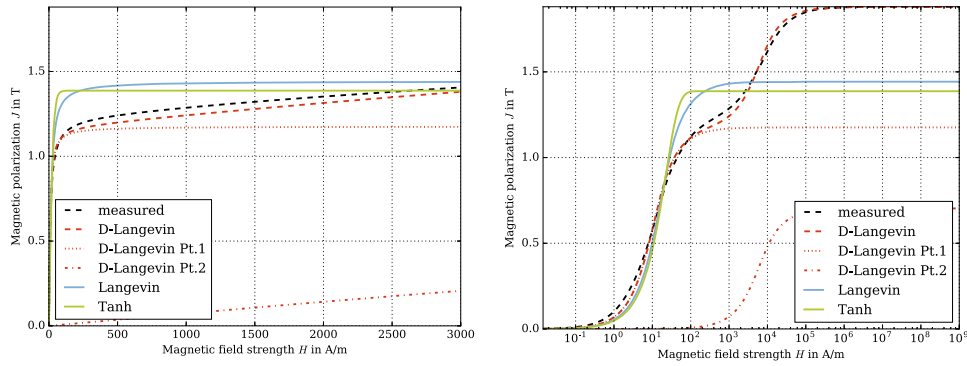


FIG. 5. Comparison of measured (black dashed line) and modelled anhysteretic magnetization curves of grade JNEX-900. (a) Normal scaling and (b) log-scale on abscissa. In addition, the two components of the double Langevin function (Pt. 1 and 2) are shown.

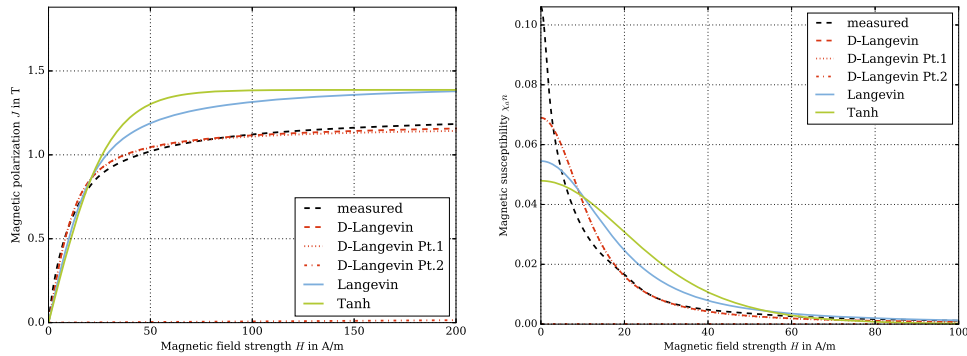


FIG. 6. Comparison of measured (black dashed line) and modelled anhysteretic magnetization curves of grade JNEX-900. (a) Zoom of Fig. 1 and (b) magnetic susceptibility. In addition, the two components of the double Langevin function (Pt. 1 and 2) are shown.

grades the share of the two Langevin functions is slightly different, that is the proportion of the second part ( $J_{s,b}$ ) grows.

In addition, to the three non-oriented electrical steel grades the match of the different parametric saturation curves with the measured anhysteretic curve of a grain-oriented material, B23P090, with a saturation polarization of 2.05 T is studied (Figs. 7 and 8). The corresponding parameters are given in Table IV. An excellent match is obtained with the double Langevin function over the whole magnetization range, whereas the classical Langevin- and tanh-function are either applicable at low to medium magnetic polarization levels, i.e., 1.2 T, or in the saturation region. It is apparent that the distinction between the two different passages in the magnetization process is less pronounced than in case of non-oriented materials, i.e., the characteristic fields of both parts are closer and, in general smaller. This is in accordance with the different magnetization process in grain oriented materials.

TABLE III. Parameters of the Anhysteretic Function for Grade JNEX-900.

$f_{an}$	$J_{s,a}$ in T	$H_{0,a}$ in A/m	$J_{s,b}$ in T	$H_{0,b}$ in A/m
Langevin	1.44259	8.8146	–	–
Tanh	1.38705	28.941	–	–
Double Langevin	1.1758	5.67589	0.703262	3218.93

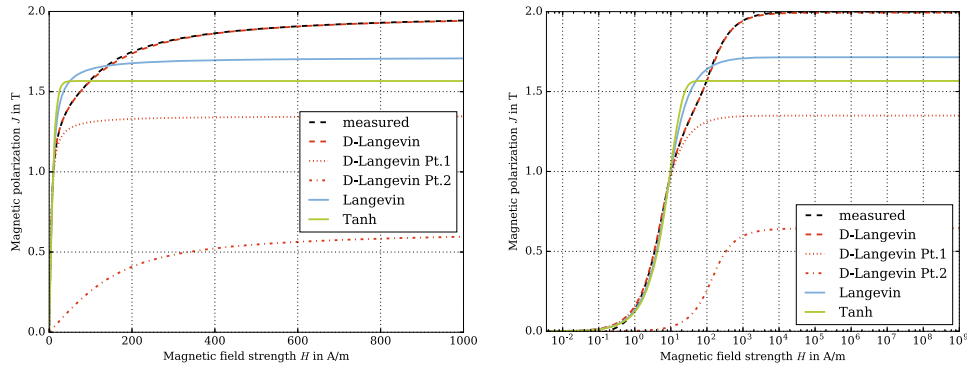


FIG. 7. Comparison of measured (black dashed line) and modelled anhysteretic magnetization curves of grade B23P090. (a) Normal scaling and (b) log-scale on abscissa. In addition, the two components of the double Langevin function (Pt. 1 and 2) are shown.

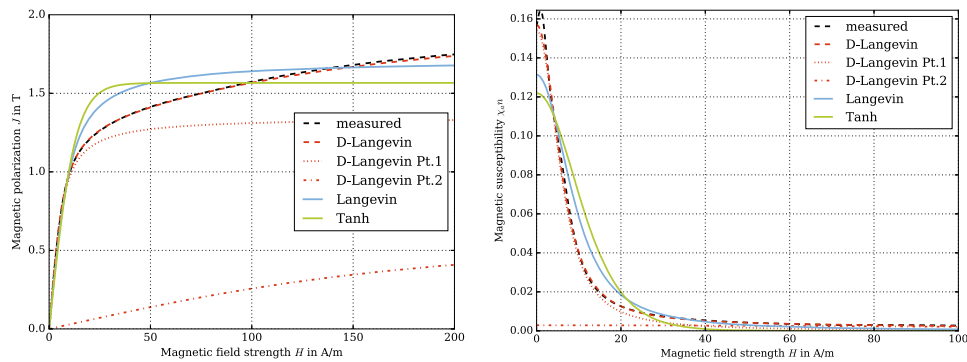


FIG. 8. Comparison of measured (black dashed line) and modelled anhysteretic magnetization curves of grade B23P090. (a) Zoom of Fig. 1 and (b) magnetic susceptibility. In addition, the two components of the double Langevin function (Pt. 1 and 2) are shown.

TABLE IV. Parameters of the Anhysteretic Function for Grade B23P090.

$f_{an}$	$J_{s,a}$ in T	$H_{0,a}$ in A/m	$J_{s,b}$ in T	$H_{0,b}$ in A/m
Langevin	1.71466	4.33737	–	–
Tanh	1.56633	12.8244	–	–
Double Langevin	1.3496	2.89673	0.644288	75.1064

#### IV. CONCLUSION

The aim of this work is to study the accuracy of the Langevin- and tanh-function, which can be derived from the Brillouin functions, to represent the anhysteretic magnetization curve. This truly reversible magnetization curve is central to the modeling of magnetic hysteresis and, in particular, to a physical-based parameter identification process.<sup>4</sup> It turns out that both are less appropriate to model the anhysteretic curve. For this reason and the observation of two passages in the anhysteretic magnetization curve, two Langevin functions are superposed in Refs. 6 and 7. Thereby one additional degree of freedom is introduced, whereas the sum of the two saturation values is constrained to the saturation polarization calculated from the alloy content. In this paper, a detailed study of the three different parametric saturation curves and their match with four different measured anhysteretic curves is presented. Parameters to describe the anhysteretic curves are given. An excellent match along the complete magnetic polarization range is obtained. This allows then to develop a physical-based and, in particular, more stable parameter identification of the Jiles-Atherton and GRUCAD hysteresis

model as well as an improved accuracy in the modeling of static and dynamic hysteresis loops over the whole polarization range. Further on, valuable information on the different magnetization process at play can be acquired analyzing the parameters and share of the two different Langevin functions.

<sup>1</sup> D. C. Jiles and D. L. Atherton, *J. Magn. Magn. Mater.* **61**(1), 48 (1986).

<sup>2</sup> P. Koltermann, L. Righi, J. Bastos, R. Carlson, N. Sadowski, and N. Batistela, *Phys. B, Condensed Matter* **275**, 233 (2000).

<sup>3</sup> E. Kokornaczyk and M. Gutowski, *Magn. IEEE Trans.* **51**(2), 1 (2015).

<sup>4</sup> S. Steentjes, M. Petrun, D. Dolinar, and K. Hameyer, *Magn. IEEE Trans.* **52**(5), 1 (2016).

<sup>5</sup> R. G. Harrison, *Magn. IEEE Trans.* **48**(3), 1115–1129 (2012).

<sup>6</sup> S. Steentjes, F. Henrotte, C. Geuzaine, and K. Hameyer, *Intern. J. Numer. Model.* **27**(3) (2014).

<sup>7</sup> S. Steentjes, D. Eggers, and K. Hameyer, *Magn. IEEE Trans.* **48**(11) (2012).